

Ubiquity of the quantum boomerang effect in Hermitian Anderson-localized systems

Flavio Noronha¹ and Tommaso Macrì^{2,1}

¹Departamento de Física Teórica e Experimental, Universidade Federal do Rio Grande do Norte, Campus Universitário, Lagoa Nova, Natal-RN 59078-970, Brazil

²ITAMP, Harvard-Smithsonian Center for Astrophysics, Cambridge, Massachusetts 02138, USA

(Dated: August 1, 2022)

A particle with finite initial velocity in a disordered potential comes back and in average stops at the original location. This phenomenon dubbed ‘quantum boomerang effect’ (QBE) has been recently observed in an experiment simulating the quantum kicked-rotor model [Phys. Rev. X **12**, 011035 (2022)]. We provide analytical arguments that support QBE in a wide class of disordered systems. Sufficient conditions to observe the *real-space* QBE effect are (*a*) Anderson localization, (*b*) the reality of the spectrum for the case of non-Hermitian systems, (*c*) the ensemble of disorder realizations $\{H\}$ be invariant under the application of \mathcal{RT} , and (*d*) the initial state is an *eigenvector* of \mathcal{RT} , where \mathcal{R} is a reflection $x \rightarrow -x$ and \mathcal{T} is the time-reversal operator. The QBE can be observed in *momentum-space* in systems with dynamical localization if conditions (*c*) and (*d*) are satisfied with respect to the operator \mathcal{T} instead of \mathcal{RT} . These conditions allow the observation of the QBE in *time-reversal* symmetry broken models, contrarily to what was expected from previous analyses of the effect, and in a large class of non-Hermitian models. We provide examples of QBE in lattice models with magnetic flux breaking time-reversal symmetry and in a model with electric field. Whereas the QBE straightforwardly applies to noninteracting many-body systems, we argue that a real-space (momentum-space) QBE is absent in weakly interacting bosonic systems due to the breaking of RT (T) symmetry.

Introduction. The presence of disorder in a medium may lead to Anderson localization (AL) of quantum particles due to destructive interference [1]. AL has been experimentally observed in many platforms, including light [2, 3], ultrasound waves [4] and atomic matter [5–9]. AL appears not only in Hermitian systems, but also in non-Hermitian models [10–37], which can be experimentally implemented with several platforms [38–40].

One of the consequences of AL in the transport properties of a system is the quantum boomerang effect (QBE). It was theoretically shown that in the Anderson model the disorder-averaged center of mass (DACM) of a particle launched with a finite momentum k_0 would initially propagate ballistically, make a U-turn toward the origin after some time and stop at the initial position [41]. This phenomenon is different from the behavior expected for classical particles, where the center of mass would initially move away from the origin and saturate at a distance ℓ of the order of the mean free path.

In Ref. [42] it was found that mean-field interactions in the Anderson model lead to the partial destruction of the QBE in the sense that the DACM stops after the U-turn, before reaching the origin. Recently, the presence of QBE was numerically shown in several *T*-symmetric systems, including quasicrystals, models with disorder in the hoppings and in the quantum kicked rotor (QKR) [43]. The QKR presents AL and QBE in momentum space in the absence of interactions [43, 44]. When interactions are present, dynamical localization is destroyed [45]. The existence of the QBE was confirmed in a very recent experimental implementation of the QKR [46]. The authors also showed the important role of time-reversal symmetry in that particular system, Floquet gauge and the initial state symmetry in supporting or disrupting the QBE. By using stochastic kicking in order to destroy AL, it was

shown the breakdown of QBE. Moreover, all the previous results leading to the QBE were found in Hermitian *T*-symmetric systems. Several questions arise as consequence of those findings, especially concerning the most general conditions to observe the QBE.

In this work we provide analytical arguments for the presence of the QBE in a class of Hamiltonians much broader than the *T*-symmetric ones, including both Hermitian and non-Hermitian models. We illustrate the validity of our analytical findings by means of numerical investigations showing the QBE in several models.

Conditions for the QBE. For compactness of notation, we consider here one-dimensional single-particle models. However, all the considerations below can be immediately generalized to an arbitrary number of spatial dimensions and many-body systems. We consider a Hamiltonian H that may be either Hermitian or non-Hermitian. In the following, \mathcal{T} is the time reversal operator and \mathcal{R} is the reflection operator $\mathcal{R} : x \rightarrow -x$. We will show that the QBE is expected to appear in real space if (*a*) the Hamiltonian presents AL, (*b*) all eigenenergies are real, (*c*) the ensemble $\{H\}$ of all disorder realizations of the model is RT invariant, $\mathcal{RT}\{H\}(\mathcal{RT})^{-1} = \{H\}$, and (*d*) the initial state is an eigenstate of \mathcal{RT} , $\mathcal{RT}|\psi_0\rangle = \pm|\psi_0\rangle$.

Without loss of generality we assume that the center of mass of the initial wave packet is positioned at the origin. We can expand $|\psi_0\rangle = \sum_n c_n |\phi_n\rangle$ in terms of the eigenvectors of the Hamiltonian, $H|\phi_n\rangle = \epsilon_n |\phi_n\rangle$. Using condition (*b*) we find that, at an arbitrary time t , the center of mass is given by

$$\langle x(t) \rangle = \sum_{n,m} c_n c_m^* \exp[-i(\epsilon_n - \epsilon_m)t] \langle \phi_m | X | \phi_n \rangle, \quad (1)$$

where X is the position operator. Using condition (*a*) we have, after averaging over many disorder realizations and

taking the limit $t \rightarrow +\infty$, the diagonal ensemble [41, 46, 47]

$$\overline{\langle x(+\infty) \rangle} = \sum_n \overline{|c_n|^2 \langle \phi_n | X | \phi_n \rangle}, \quad (2)$$

where the overline $(\overline{\dots})$ denotes average over the disorder realizations. An equivalent expression is found when one takes the limit $t \rightarrow -\infty$ and hence

$$\overline{\langle x(+\infty) \rangle} = \overline{\langle x(-\infty) \rangle}. \quad (3)$$

For each disorder realization H we define its RT counterpart $\tilde{H} = \mathcal{R}TH(\mathcal{R}T)^{-1}$. The center of mass of a state evolved under the disorder realization H satisfies

$$\begin{aligned} \langle x(t) \rangle_H &= (\pm \langle \psi_0 |) [\mathcal{R}T \exp(iH^\dagger t) (\mathcal{R}T)^{-1}] [\mathcal{R}TX(\mathcal{R}T)^{-1}] \\ &\quad \times [\mathcal{R}T \exp(-iHt) (\mathcal{R}T)^{-1}] (\pm | \psi_0 \rangle) \\ &= -\langle x(-t) \rangle_{\tilde{H}}, \end{aligned} \quad (4)$$

where we have used condition (d). Now we use condition (c), which is equivalent to say that for each disorder realization H its RT counterpart \tilde{H} is also a disorder realization of the same model. Therefore $\overline{\langle x(t) \rangle} = -\overline{\langle x(-t) \rangle}$ and, in particular,

$$\overline{\langle x(+\infty) \rangle} = -\overline{\langle x(-\infty) \rangle}. \quad (5)$$

From Eqs. (3) and (5) we have $\overline{\langle x(+\infty) \rangle} = 0$, which guarantees that the QBE occurs.

In higher dimensions, without loss of generality, the initial momentum is chosen to be aligned along the X direction and \mathcal{R} is the reflection with respect to X . In cases where conditions (c) and (d) are not satisfied with respect to the operator $\mathcal{R}T$ it is still possible to guarantee the QBE if there is some unitary operator \mathcal{U} that commutes with X and causes conditions (c) and (d) to be satisfied with respect to $\mathcal{U}\mathcal{R}T$ [see the Supplemental Material (SM) [48] for details on the derivation]. In models that present localization in momentum space, e.g. the QKR, the QBE can appear in $\langle p(t) \rangle$ [43, 46]. The demonstration of this effect in momentum space follows the arguments that we have shown above but considers only the operator \mathcal{T} instead of $\mathcal{R}T$ in conditions (c) and (d) (see SM [48]). In the following we show numerically the QBE in several Hermitian models in which the presented analytical arguments apply. In Ref. [49] we confirm numerically the QBE in several non-Hermitian models and show its main features in those systems.

QBE in models with magnetic field. In this section we show the QBE in two different models that break T symmetry by means of a magnetic field, the Harper-Hofstadter ladder model and the 2D Harper model. In order to demonstrate the QBE in a minimal model that breaks T symmetry we consider first the Harper-Hofstadter ladder model [50–53], illustrated in Fig. 1(a) and described by the Hamiltonian

$$\begin{aligned} H &= -J \sum_i [e^{i\phi/2} (b_i^\dagger b_{i+1} + a_{i+1}^\dagger a_i) + H.c.] \\ &\quad - \Omega \sum_i [a_i^\dagger b_i + H.c.] + \sum_i \epsilon_{a,i} a_i^\dagger a_i + \epsilon_{b,i} b_i^\dagger b_i, \end{aligned} \quad (6)$$

where $i = 1, \dots, N$, N is the number of sites in each of the chains A and B , and a_i^\dagger (b_i^\dagger) creates a particle on site i of chain A (B). $Je^{\pm i\phi/2}$ characterize the intra-chain hoppings, where $J, \phi \in \mathbb{R}$, while $\Omega \in \mathbb{R}$ is the inter-chain hopping amplitude. We consider open boundary conditions in each chain. The onsite potentials $\epsilon_{a,i}, \epsilon_{b,i}$ are uncorrelated random numbers sampled from a uniform distribution over $[-W/2, W/2]$. The model presents Anderson localization due to the disorder.

Here we define the reflection operator as $\mathcal{R} : (a_i, b_i) \rightarrow (a_{-i}, b_{-i})$ and the time-reversal operator $\mathcal{T} = \mathcal{K}$ is the complex conjugation. Decomposing the Hamiltonian $H = H_0 + H_1$ into a hopping term H_0 and a local potential term H_1 , one can check that H_0 breaks time-reversal symmetry due to the complex hoppings $Je^{\pm i\phi/2}$. This symmetry breaking is related to a magnetic flux through each plaquette of the ladder, which is proportional to the phase ϕ acquired along the loop around each plaquette. The hopping term satisfies $\mathcal{R}TH_0(\mathcal{R}T)^{-1} = H_0$. The ensemble of disorder realizations is RT invariant, $\mathcal{R}T\{H\}(\mathcal{R}T)^{-1} = \{H\}$. Therefore the QBE is expected to appear if condition (d) is satisfied.

A wave packet of the system may be written as a spinor with components in chains A and B , in the form $\psi(x_j) = (\psi^{(a)}(x_j), \psi^{(b)}(x_j))$. We define four wave packets

$$\begin{aligned} \psi_{0\pm}(x_j) &= \mathcal{N}_0 \exp(-x_j^2/2\sigma^2 + ik_0 x_j) (1, \pm 1), \\ \psi_{1\pm}(x_j) &= \mathcal{N}_1 x_j \exp(-x_j^2/2\sigma^2 + ik_0 x_j) (1, \pm 1), \end{aligned} \quad (7)$$

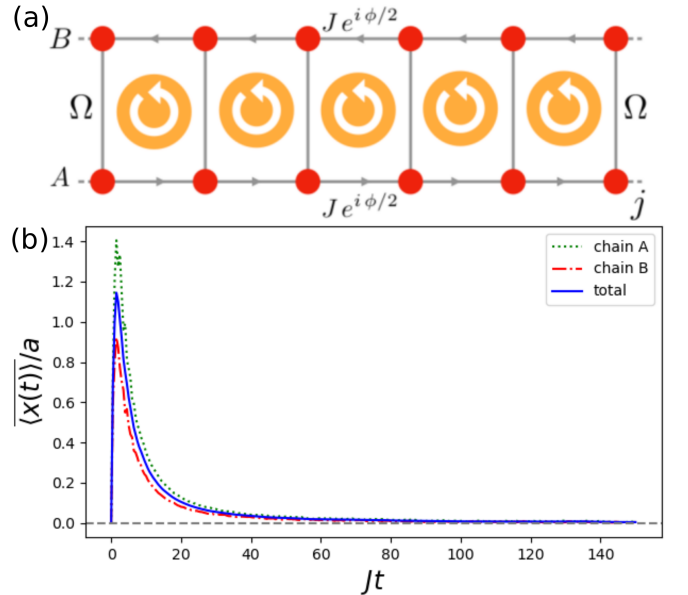


Figure 1. QBE with broken T symmetry: The Harper-Hofstadter ladder. (a) Two-leg ladder model with magnetic flux ϕ per plaquette, intra-chain complex hopping $Je^{\pm i\phi/2}$ and inter-chain coupling Ω . (b) Disorder averaged center of mass in chain A (green dotted), chain B (red dash-dotted) and averaged in the whole system (blue solid). We set $\Omega/J = 2$, $W/J = 6$, $\phi = (\pi/2)(\sqrt{5} - 1)/2$, $N = 4 \times 10^2$, $n_d = 5 \times 10^5$ and initial state ψ_{1+} with $\sigma/a = 10$ and $k_0a = 1.4$.

where \mathcal{N}_0 and \mathcal{N}_1 are normalization factors and x_j is the position of site j (for simplicity we consider an unitary lattice parameter $a = 1$). These wave packets satisfy $\mathcal{RT}\psi_{0\pm} = +\psi_{0\pm}$, $\mathcal{RT}\psi_{1\pm} = -\psi_{1\pm}$. As a consequence, the QBE appears in the total center of mass $\langle x(t) \rangle = \sum_i x_i [\langle \psi^{(a)}(x_i, t) \rangle^2 + \langle \psi^{(b)}(x_i, t) \rangle^2]$ using any of the four initial wave packets above [see in Fig. 1(b) the QBE using ψ_{1+}]. This shows that the initial wave function does not need to be invariant under \mathcal{RT} , but it is enough to be its eigenstate. Moreover, the QBE is present in each chain individually through $\langle x(t) \rangle_l = [\sum_i x_i \langle \psi^{(l)}(x_i, t) \rangle^2] / \sum_i \langle \psi^{(l)}(x_i, t) \rangle^2$, $l = a, b$. The validity of the QBE in each chain can be checked analytically through Eq. (4) using $\Pi_l X \Pi_l$ instead of X , where Π_l is the projection operator on chain $l = a, b$. Additional data for the Harper-Hofstadter ladder model is available in the SM [48].

The Harper-Hofstadter ladder model can also be interpreted as composed of spin-1/2 particles on a chain, and in Eq. (6) a_i^\dagger (b_i^\dagger) creates at site i a spin up (down) fermion. In this case, $\mathcal{T} = \mathcal{SK}$ takes the complex conjugate (\mathcal{K}) and flips the spin indices ($\mathcal{S} = \sigma_x$). Conditions (c)-(d) are not met with respect to the operator $\mathcal{RT} = \sigma_x \mathcal{RK}$. Therefore we choose $\mathcal{U} = \mathcal{S}^{-1}$ so the operator $\mathcal{URT} = \mathcal{RK}$ acts in the same way that it acted in the previous interpretation of the Harper-Hofstadter ladder. Therefore the ensemble of all disorder realizations satisfies $\mathcal{URT}\{H\}(\mathcal{URT})^{-1} = \{H\}$ and $\psi_{0\pm}, \psi_{1\pm}$ defined above are eigenvectors of \mathcal{URT} . This leads to the QBE, illustrating that our analytical arguments also apply in the case of particles with spin.

Here, in order to further investigate the importance of conditions (c)-(d), we consider the presence of disorder in the Harper model of a 2D lattice with an external magnetic field, given by the Hamiltonian [51, 54]

$$H = -J \sum_{j,l} [e^{-i2\pi\alpha l} c_{j+1,l}^\dagger c_{j,l} + c_{j,l+1}^\dagger c_{j,l} + H.c.] + \sum_{j,l} \epsilon_{j,l} c_{j,l}^\dagger c_{j,l}, \quad (8)$$

where $j = 1, \dots, N_x$ ($l = 1, \dots, N_y$) characterizes the x (y) coordinate of the system with lattice parameter $a = 1$ and $c_{j,l}^\dagger$ creates a particle on site (j, l) . The complex coefficients $Je^{\mp i2\pi\alpha l}$ define the hoppings in the horizontal direction and $J \in \mathbb{R}$ is the hopping in the vertical direction. α is proportional to the magnetic flux in each plaquette. We consider open boundary conditions. The onsite potentials $\epsilon_{j,l}$ are uncorrelated random numbers sampled from a uniform distribution over $[-W/2, W/2]$. Because of the disorder this model presents AL [55–60].

Here we define the reflection operators as $\mathcal{R}_x : c_{j,l} \rightarrow c_{-j,l}$, $\mathcal{R}_y : c_{j,l} \rightarrow c_{j,-l}$ and the time-reversal operator $\mathcal{T} = \mathcal{K}$ is the complex conjugation. Decomposing the Hamiltonian $H = H_0 + H_1$ into a hopping term H_0 and a local potential term H_1 , one can check that H_0 breaks time-reversal symmetry due to the complex hoppings. Though H_0 is not T symmetric, it

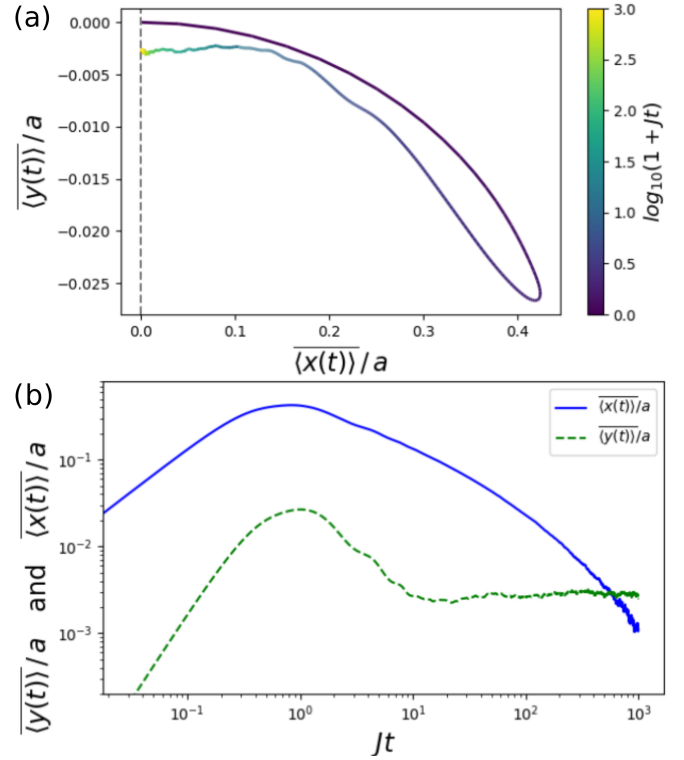


Figure 2. **QBE with broken T symmetry: The Harper model.** (a) Trajectory of $\langle x(t) \rangle \times \langle y(t) \rangle$ presenting the full (partial) boomerang effect in the direction parallel (perpendicular) to the initial momentum $\mathbf{k}_0 = k_0 \hat{x}$, i.e. $\langle x(+\infty) \rangle = 0$ ($\langle y(+\infty) \rangle \neq 0$). The color bar indicates the time propagation in the interval $Jt \in [0, 1000]$. (b) In the blue solid line we show that $\langle x(t) \rangle$ decreases and tends to vanish and in the green dashed line we show that $\langle y(t) \rangle$ remains finite at long times. We set $W/J = 10$, $\alpha = 0.02$, $n_d = 7 \times 10^5$ disorder realizations, $\sigma/a = 10$, $k_0 a = \pi/2$ and $N_x = N_y = 190$.

satisfies $\mathcal{R}_x \mathcal{T} H_0 (\mathcal{R}_x \mathcal{T})^{-1} = \mathcal{R}_y \mathcal{T} H_0 (\mathcal{R}_y \mathcal{T})^{-1} = H_0$. The ensemble of disorder realizations is RT invariant, $\mathcal{R}_x \mathcal{T}\{H\}(\mathcal{R}_x \mathcal{T})^{-1} = \mathcal{R}_y \mathcal{T}\{H\}(\mathcal{R}_y \mathcal{T})^{-1} = \{H\}$. Therefore the QBE is expected to appear if condition (d) is satisfied.

We initialize the system in a Gaussian wave packet, $\psi_0(\mathbf{r}_{j,l}) = \mathcal{N}_0 \exp(-r_{j,l}^2/2\sigma^2 + i\mathbf{k}_0 \cdot \mathbf{r}_{j,l})$, where $\mathbf{r}_{j,l}$ is the position of site (j, l) . Without loss of generality we consider $\mathbf{k}_0 = k_0 \hat{x}$. This wave function satisfies $\mathcal{R}_x \mathcal{T} \psi_0(\mathbf{r}_{j,l}) = \psi_0(\mathbf{r}_{j,l})$ and hence the QBE is expected to take place in the direction of the initial momentum, i.e. in $\langle x(t) \rangle$. In the perpendicular direction we have $\mathcal{R}_y \mathcal{T} \psi_0(\mathbf{r}_{j,l}) = \psi_0(\mathbf{r}_{j,l})^* \neq \psi_0(\mathbf{r}_{j,l})$ and our analytical arguments do not guarantee that the QBE will take place in $\langle y(t) \rangle$. We check numerically that the QBE appears in the x direction but is broken in the y direction; after the U-turn $\langle y(t) \rangle$ does not reach the origin (see Fig. 2). This confirms the presence of the QBE in T -broken models and illustrates the importance of conditions (c)-(d).

Anderson model with electric field. Another interesting case is the 1D Anderson model in the presence of an

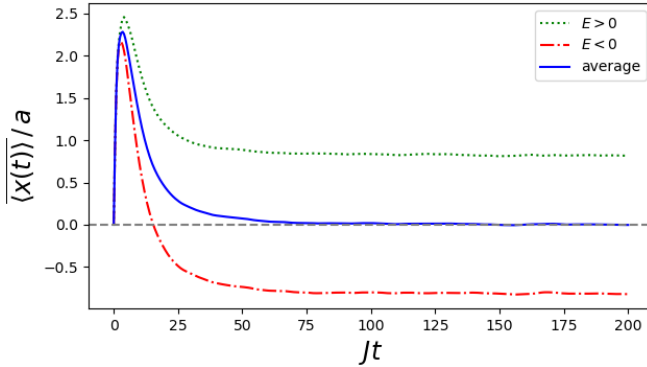


Figure 3. **QBE in the Anderson model with electric field.** Using $W/J = 3$ and $|E|/J = 0.1$, we show the disorder-averaged center of mass for the case with $E > 0$ ($E < 0$) in green dotted (red dot-dashed) line. The average of these two cases is shown in blue solid line. In these data we considered a Gaussian initial state and used $\sigma/a = 10$, $k_0a = 1.4$, $N = 4 \times 10^2$ and $n_d = 5 \times 10^4$.

external electric field E . The model reads

$$H = \sum_j \left[-Jc_{j+1}^\dagger c_j - Jc_j^\dagger c_{j+1} + (\epsilon_j - jE)c_j^\dagger c_j \right], \quad (9)$$

where ϵ_j are sampled from a uniform distribution over $[-W/2, W/2]$. The ensemble of disorder realizations with field E satisfies $\mathcal{RT}\{H(E)\}(\mathcal{RT})^{-1} = \{H(-E)\}$ and hence the QBE is not observed when averaging $\langle x(t) \rangle$ over $\{H(E)\}$ [see green dotted (red dot-dashed) line in Fig. 3 for $E > 0$ ($E < 0$)]. To guarantee $\mathcal{RT}\{H\}(\mathcal{RT})^{-1} = \{H\}$ we consider the union of the ensemble of disorder realizations with field $+E$ with the realizations with $-E$, i.e. $\{H\} = \{H(+E)\} \cup \{H(-E)\}$. Figure 3 shows in blue solid line the presence of the QBE in this case. Notice that this is not equivalent to take the average of the Hamiltonians with $E > 0$ with those with $E < 0$ and obtain the Anderson model in the absence of E . These results further illustrate the importance of condition (c).

Many-body systems. Non-interacting many-particle systems satisfying the conditions mentioned in the analytical arguments are expected to display the QBE. In fact, it is straightforward to prove that for an initial N -particle bosonic (B) or fermionic (F) state $\psi_{B,F}(x_1, \dots, x_N) = \langle x_1, \dots, x_N | \chi_1, \dots, \chi_N \rangle_{B,F}$ one has $\langle X(t) \rangle = \sum_i \langle \chi_i(t) | X_i | \chi_i(t) \rangle = \sum_i \langle x_i(t) \rangle$, where $X = \sum_i X_i$, X_i is the position operator corresponding to the i -th particle, $\langle x_i(t) \rangle$ is its center of mass and χ_i is the i -th orbital, $i = 1, \dots, N$. Therefore the QBE appears in $\langle x_i(t) \rangle$ and hence in $\langle X(t) \rangle$ averaging over disorder realizations. We also notice that, if there is a sufficiently large number N of particles far from each other, each of them feels a different local disorder in its vicinity and the summation $\sum_i \langle x_i(t) \rangle$ plays the role of average over disorder realizations. Therefore, for a single disorder realization the QBE is also expected to appear in the average center of mass of the system $\langle X(t) \rangle/N$. A similar argument holds for the QBE in momentum space. Therefore,

in the case of non-interacting many particles we expect the QBE to appear even in the presence of electric or magnetic fields if conditions (a)-(d) are met.

The presence of interactions in some disordered systems may deeply alter the nature of the Anderson transition [61]. Interactions can also lead to a breaking of the QBE effect by either destroying localization or \mathcal{RT} symmetry. Weakly interacting Bose gases with a contact potential $U(\mathbf{r}) = g \delta(\mathbf{r})$ are described within a mean-field Hamiltonian density $H = H_0 + g|\psi(\mathbf{r}, t)|^2$, where H_0 contains the kinetic and the local disordered potential. The nonlinear term breaks both \mathcal{T} and \mathcal{RT} symmetries, leading to the absence of QBE both in momentum and real space. This is in agreement with the analysis in [42] for the 1D Gross-Pitaevskii equation (GPE). In the following we investigate the QKR model, which presents localization in momentum space and hence displays the QBE in $\langle p(t) \rangle$ in the non-interacting case [43, 44, 46]. In Fig. 4 we show the dynamics of $\langle p(t) \rangle$ for the QKR with contact interactions. The mean-field bosonic QKR is governed by the GPE

$$i\bar{k}\partial_t\psi = -\bar{k}^2 \frac{\partial_x^2\psi}{2} + g|\psi|^2\psi + K \cos(x) \sum_{n=-\infty}^{\infty} \delta(t-n-\alpha)\psi. \quad (10)$$

We solve it using third order split-step Fourier method.

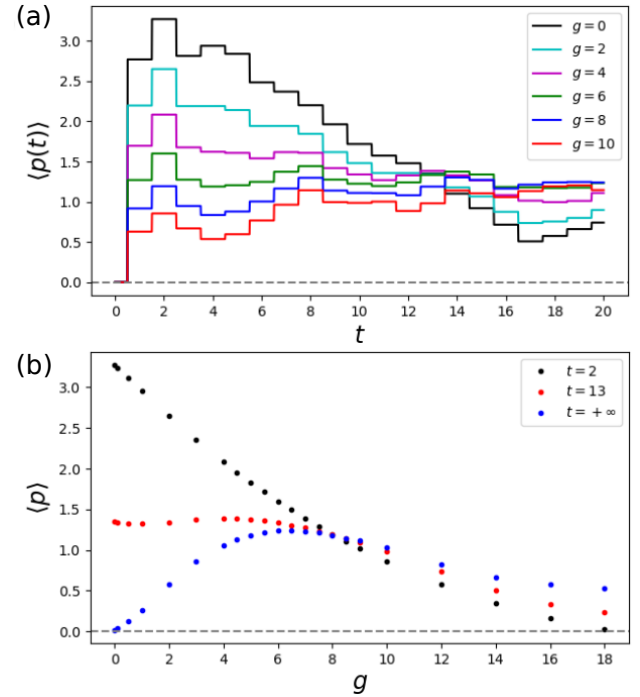


Figure 4. **QBE in the interacting quantum kicked-rotor model.** (a) Short-time momentum average for different interaction strengths. (b) Asymptotic momentum average (blue), momentum at $t = 2$ (black), and average momentum at $t = 13$ (red). For both plots we set $\alpha = 0.5$, $K = 5$, $x_0 = \pi/2$, $\sigma_k = 3$, $\bar{k} = 1$, size of the system $L = 2\pi \times 512$, discretization in real space $\Delta x = 2\pi/1024$ and in time $\Delta t = 10^{-2}$.

The initial wave packet is a Gaussian in momentum space with variance σ_k and initial “boost” x_0 , $\psi_0(p) = \mathcal{N} \exp(-p^2/2\sigma_k^2 - ix_0 p)$.

Interactions are known to destroy dynamical localization in the QKR [45]. Furthermore any finite interaction g breaks T symmetry, and hence the *full* QBE is present only for $g = 0$. However, $\langle p(t) \rangle$ still displays a *partial* boomerang with a U-turn at $t = 2$ for $0 < g < g_c \approx 8$. Beyond this critical interaction, there is no signature of the QBE and $\langle p \rangle_{t=2} < \langle p \rangle_{t=\infty}$, where we compute $\langle p \rangle_{t=\infty}$ as an average of $\langle p(t) \rangle$ in the interval $t \in [500, 1000]$. This same behavior is observed for other values of K (see the SM [48] for additional data).

Summary. While the QBE was previously found only in T -symmetric Hermitian systems with restricted initial conditions, we showed that QBE can be observed for a wide class of Hamiltonians breaking T symmetry and hermiticity, and in a variety of initial states. The QBE is expected to be present in systems of any dimension d and any number N of noninteracting particles. It was shown that sufficient conditions to observe the QBE are (a) Anderson localization, (b) reality of eigenenergies, (c) reflection-time invariance of the ensemble $\{H\}$ of disorder realizations and (d) the initial wave function be an eigenstate of the reflection-time operator. We observe the breakdown of the QBE when these conditions are not met. However, these conditions are quite general and hence our results demonstrate the ubiquity of the QBE in localized systems. It is an open question whether these conditions can be further generalized. We emphasize that the examples discussed in this work have a direct implementation in ultracold systems. Harper-Hofstadter ladders have been realized in e.g. [62] with laser-induced hopping along synthetic dimensions and a complex hopping along the chains producing an effective magnetic field. Local disorder can be added by superimposing an additional incommensurate

lattice as in [63] or with a speckle potential [7]. Although in the numerical investigations we focused on Hermitian models, the QBE holds for a broad class of non-Hermitian systems [49]. Finally, we provided arguments for which mean-field interactions prohibit QBE in bosonic systems. The question whether many-body localized (MBL) phases in interacting systems display QBE remains open [64, 65]. Interestingly, Creutz ladders with cross tunnelings can lead to the formation of flat bands and might display disorderless MBL states [66–69]. Also, the presence of momentum-space QBE can be tested in the interacting kicked-rotor model tuning the interaction in a ^7Li BEC via Feshbach resonances [45, 46].

While we were finishing this manuscript we learned about the recent work of Ref. [70], which has partial overlap with our findings. The authors study a 1D model with spin-orbit coupling and briefly mention the sufficient conditions to observe the QBE. While our analytical derivation have some similarity with the arguments presented in [70], our derivation is more general in the sense that we demonstrate the QBE: (i) in non-Hermitian systems with real spectrum, (ii) in a broader class of initial states and (iii) in cases where H_0 is not RT symmetric if the ensemble $\{H_0\}$ is RT invariant. This last point is relevant e.g. in the model with electric field and in the Hatano-Nelson model [49].

Acknowledgments. We acknowledge L. Tessieri, P. Vignolo, and J. A. S. Lourenço for useful discussions. We thank N. Cheroret and D. Delande for useful feedback on the manuscript. T.M. acknowledges CNPq for support through Bolsa de produtividade em Pesquisa n.311079/2015-6. This work was supported by the Serapilheira Institute (grant number Serra-1812-27802). We thank the High Performance Computing Center (NPAD) at UFRN for providing computational resources.

[1] P. W. Anderson, Absence of diffusion in certain random lattices, *Phys. Rev.* **109**, 1492 (1958).

[2] A. A. Chabanov, M. Stoytchev, and A. Z. Genack, Statistical signatures of photon localization, *Nature* **404**, 850 (2000).

[3] T. Schwartz, G. Bartal, S. Fishman, and M. Segev, Transport and anderson localization in disordered two-dimensional photonic lattices, *Nature* **446**, 52 (2007).

[4] H. Hu, A. Strybulevych, J. Page, S. E. Skipetrov, and B. A. van Tiggelen, Localization of ultrasound in a three-dimensional elastic network, *Nature Physics* **4**, 945 (2008).

[5] J. Chabé, G. Lemarié, B. Grémaud, D. Delande, P. Sriftgiser, and J. C. Garreau, Experimental observation of the anderson metal-insulator transition with atomic matter waves, *Phys. Rev. Lett.* **101**, 255702 (2008).

[6] I. Manai, J.-F. Clément, R. Chicireanu, C. Hainaut, J. C. Garreau, P. Sriftgiser, and D. Delande, Experimental observation of two-dimensional anderson localization with the atomic kicked rotor, *Phys. Rev. Lett.* **115**, 240603 (2015).

[7] J. Billy, V. Josse, Z. Zuo, A. Bernard, B. Hambrecht, P. Lugan, D. Clément, L. Sanchez-Palencia, P. Bouyer, and A. Aspect, Direct observation of anderson localization of matter waves in a controlled disorder, *Nature* **453**, 891 (2008).

[8] F. Jendrzejewski, A. Bernard, K. Mueller, P. Cheinet, V. Josse, M. Piraud, L. Pezzé, L. Sanchez-Palencia, A. Aspect, and P. Bouyer, Three-dimensional localization of ultracold atoms in an optical disordered potential, *Nature Physics* **8**, 398 (2012).

[9] G. Semeghini, M. Landini, P. Castilho, S. Roy, G. Spagnolli, A. Trenkwalder, M. Fattori, M. Inguscio, and G. Modugno, Measurement of the mobility edge for 3d anderson localization, *Nature Physics* **11**, 554 (2015).

[10] N. Hatano and D. R. Nelson, Localization transitions in non-hermitian quantum mechanics, *Phys. Rev. Lett.* **77**, 570 (1996).

[11] N. Hatano and D. R. Nelson, Vortex pinning and non-hermitian quantum mechanics, *Phys. Rev. B* **56**, 8651 (1997).

[12] N. Hatano and D. R. Nelson, Non-hermitian delocalization and eigenfunctions, *Phys. Rev. B* **58**, 8384 (1998).

[13] K. B. Efetov, Directed quantum chaos, *Phys. Rev. Lett.* **79**, 491 (1997).

[14] J. Feinberg and A. Zee, Non-hermitian random matrix theory: Method of hermitian reduction, *Nuclear Physics B* **504**, 579 (1997).

[15] J. Feinberg and A. Zee, Non-hermitian localization and delocalization, *Phys. Rev. E* **59**, 6433 (1999).

[16] P. W. Brouwer, P. G. Silvestrov, and C. W. J. Beenakker, Theory of directed localization in one dimension, *Phys. Rev. B* **56**, R4333 (1997).

[17] I. Y. Goldsheid and B. A. Khoruzhenko, Distribution of eigenvalues in non-hermitian anderson models, *Phys. Rev. Lett.* **80**, 2897 (1998).

[18] D. R. Nelson and N. M. Shnerb, Non-hermitian localization and population biology, *Phys. Rev. E* **58**, 1383 (1998).

[19] A. Amir, N. Hatano, and D. R. Nelson, Non-hermitian localization in biological networks, *Phys. Rev. E* **93**, 042310 (2016).

[20] C. Mudry, B. D. Simons, and A. Altland, Random dirac fermions and non-hermitian quantum mechanics, *Phys. Rev. Lett.* **80**, 4257 (1998).

[21] T. Fukui and N. Kawakami, Breakdown of the mott insulator: Exact solution of an asymmetric hubbard model, *Phys. Rev. B* **58**, 16051 (1998).

[22] I. V. Yurkevich and I. V. Lerner, Delocalization in an open one-dimensional chain in an imaginary vector potential, *Phys. Rev. Lett.* **82**, 5080 (1999).

[23] S. Longhi, D. Gatti, and G. D. Valle, Robust light transport in non-hermitian photonic lattices, *Scientific Reports* **5**, 2045 (2015).

[24] Q.-B. Zeng, S. Chen, and R. Lü, Anderson localization in the non-hermitian aubry-andré-harper model with physical gain and loss, *Phys. Rev. A* **95**, 062118 (2017).

[25] A. McDonald, T. Pereg-Barnea, and A. A. Clerk, Phase-dependent chiral transport and effective non-hermitian dynamics in a bosonic kitaev-majorana chain, *Phys. Rev. X* **8**, 041031 (2018).

[26] Z. Gong, Y. Ashida, K. Kawabata, K. Takasan, S. Higashikawa, and M. Ueda, Topological phases of non-hermitian systems, *Phys. Rev. X* **8**, 031079 (2018).

[27] R. Hamazaki, K. Kawabata, and M. Ueda, Non-hermitian many-body localization, *Phys. Rev. Lett.* **123**, 090603 (2019).

[28] H. Jiang, L.-J. Lang, C. Yang, S.-L. Zhu, and S. Chen, Interplay of non-hermitian skin effects and anderson localization in nonreciprocal quasiperiodic lattices, *Phys. Rev. B* **100**, 054301 (2019).

[29] Q.-B. Zeng, Y.-B. Yang, and Y. Xu, Topological phases in non-hermitian aubry-andré-harper models, *Phys. Rev. B* **101**, 020201(R) (2020).

[30] K. Kawabata and S. Ryu, Nonunitary scaling theory of non-hermitian localization, *Phys. Rev. Lett.* **126**, 166801 (2021).

[31] V. Freilikher, M. Pustilnik, and I. Yurkevich, Effect of absorption on the wave transport in the strong localization regime, *Phys. Rev. Lett.* **73**, 810 (1994).

[32] C. W. J. Beenakker, J. C. J. Paasschens, and P. W. Brouwer, Probability of reflection by a random laser, *Phys. Rev. Lett.* **76**, 1368 (1996).

[33] J. C. J. Paasschens, T. S. Misirpashaev, and C. W. J. Beenakker, Localization of light: Dual symmetry between absorption and amplification, *Phys. Rev. B* **54**, 11887 (1996).

[34] N. A. Bruce and J. T. Chalker, Multiple scattering in the presence of absorption: a theoretical treatment for quasi one-dimensional systems, *Journal of Physics A: Mathematical and General* **29**, 3761 (1996).

[35] S. Longhi, Topological phase transition in non-hermitian quasicrystals, *Phys. Rev. Lett.* **122**, 237601 (2019).

[36] A. F. Tzortzakakis, K. G. Makris, and E. N. Economou, Non-hermitian disorder in two-dimensional optical lattices, *Phys. Rev. B* **101**, 014202 (2020).

[37] Y. Huang and B. I. Shklovskii, Anderson transition in three-dimensional systems with non-hermitian disorder, *Phys. Rev. B* **101**, 014204 (2020).

[38] Z. Gong, Y. Ashida, K. Kawabata, K. Takasan, S. Higashikawa, and M. Ueda, Topological phases of non-hermitian systems, *Phys. Rev. X* **8**, 031079 (2018).

[39] S. Schiffer, X.-J. Liu, H. Hu, and J. Wang, Anderson localization transition in a robust \mathcal{PT} -symmetric phase of a generalized aubry-andré model, *Phys. Rev. A* **103**, L011302 (2021).

[40] W. Sebastian, M. Kremer, S. Longhi, and A. Szameit, Topological triple phase transition in non-hermitian floquet quasicrystals, *Nature* **601**, 354 (2022).

[41] T. Prat, D. Delande, and N. Cherroret, Quantum boomeranglike effect of wave packets in random media, *Phys. Rev. A* **99**, 023629 (2019).

[42] J. Janarek, D. Delande, N. Cherroret, and J. Zakrzewski, Quantum boomerang effect for interacting particles, *Phys. Rev. A* **102**, 013303 (2020).

[43] L. Tessieri, Z. Akdeniz, N. Cherroret, D. Delande, and P. Vignolo, Quantum boomerang effect: Beyond the standard anderson model, *Phys. Rev. A* **103**, 063316 (2021).

[44] S. Fishman, D. R. Grempel, and R. E. Prange, Chaos, quantum recurrences, and anderson localization, *Phys. Rev. Lett.* **49**, 509 (1982).

[45] A. Cao, R. Sajjad, H. Mas, E. Q. Simmons, J. L. Tanlimco, E. Nolasco-Martinez, T. Shimasaki, H. E. Kondakci, V. Galitski, and D. M. Weld, Interaction-driven breakdown of dynamical localization in a kicked quantum gas (2021), [arXiv:2106.09698](https://arxiv.org/abs/2106.09698).

[46] R. Sajjad, J. L. Tanlimco, H. Mas, A. Cao, E. Nolasco-Martinez, E. Q. Simmons, F. L. N. Santos, P. Vignolo, T. Macri, and D. M. Weld, Observation of the quantum boomerang effect, *Phys. Rev. X* **12**, 011035 (2022).

[47] For each disorder realization $\langle x(t) \rangle$ presents fluctuations with time due to the off-diagonal terms of Eq. (1) and they oscillate about a time-independent component given by the diagonal terms. Performing the average over disorder realizations at long times causes these time-dependent terms to cancel one another due to the random-like nature of the factors that appear in that expression.

[48] See supplemental material for more details on the analytical arguments on the quantum boomerang effect, additional numerical data for the quantum kicked rotor and for the harper-hofstadter ladder.

[49] F. Noronha, J. A. S. Lourenço, and T. Macrì, Robust quantum boomerang effect in non-hermitian systems (2022), [arXiv:2206.02922](https://arxiv.org/abs/2206.02922).

[50] P. G. Harper, The general motion of conduction electrons in a uniform magnetic field, with application to the diamagnetism of metals, *Proceedings of the Physical Society. Section A* **68**, 879 (1955).

[51] D. R. Hofstadter, Energy levels and wave functions of

bloch electrons in rational and irrational magnetic fields, *Phys. Rev. B* **14**, 2239 (1976).

[52] P. Streda, Quantised hall effect in a two-dimensional periodic potential, *Journal of Physics C: Solid State Physics* **15**, L1299 (1982).

[53] X. Wu, F. Yang, S. Yang, K. Mølmer, T. Pohl, M. K. Tey, and L. You, Synthesizing gauge fields via multicolor dressing of rydberg-atom arrays (2022), [arXiv:2203.03994](https://arxiv.org/abs/2203.03994).

[54] P. G. Harper, Single band motion of conduction electrons in a uniform magnetic field, *Proceedings of the Physical Society. Section A* **68**, 874 (1955).

[55] E. Abrahams, P. W. Anderson, D. C. Licciardello, and T. V. Ramakrishnan, Scaling theory of localization: Absence of quantum diffusion in two dimensions, *Phys. Rev. Lett.* **42**, 673 (1979).

[56] P. A. Lee and T. V. Ramakrishnan, Disordered electronic systems, *Rev. Mod. Phys.* **57**, 287 (1985).

[57] B. Kramer and A. MacKinnon, Localization: theory and experiment, *Reports on Progress in Physics* **56**, 1469 (1993).

[58] F. Wegner, Four-loop-order β -function of nonlinear σ -models in symmetric spaces, *Nuclear Physics B* **316**, 663 (1989).

[59] A. MacKinnon and B. Kramer, The scaling theory of electrons in disordered solids: Additional numerical results, *Zeitschrift für Physik B Condensed Matter* **53**, 1 (1983).

[60] K. Müller, B. Mehlig, F. Milde, and M. Schreiber, Statistics of wave functions in disordered and in classically chaotic systems, *Phys. Rev. Lett.* **78**, 215 (1997).

[61] N. Cherroret, B. Vermersch, J. C. Garreau, and D. Delande, How nonlinear interactions challenge the three-dimensional anderson transition, *Phys. Rev. Lett.* **112**, 170603 (2014).

[62] M. Mancini, G. Pagano, G. Cappellini, L. Livi, M. Rider, J. Catani, C. Sias, P. Zoller, M. Inguscio, M. Dalmonte, *et al.*, Observation of chiral edge states with neutral fermions in synthetic hall ribbons, *Science* **349**, 1510 (2015).

[63] B. Deissler, M. Zaccanti, G. Roati, C. D'Errico, M. Fattori, M. Modugno, G. Modugno, and M. Inguscio, Delocalization of a disordered bosonic system by repulsive interactions, *Nature physics* **6**, 354 (2010).

[64] J. M. Zhang, C. Shen, and W. M. Liu, Quantum quench dynamics of the bose-hubbard model at finite temperatures, *Phys. Rev. A* **83**, 063622 (2011).

[65] J. M. Zhang, C. Shen, and W. M. Liu, Strong thermalization of the two-component bose-hubbard model at finite temperatures, *Phys. Rev. A* **85**, 013637 (2012).

[66] M. Creutz, End states, ladder compounds, and domain-wall fermions, *Phys. Rev. Lett.* **83**, 2636 (1999).

[67] J. Zurita, C. E. Creffield, and G. Platero, Topology and interactions in the photonic creutz and creutz-hubbard ladders, *Advanced Quantum Technologies* **3**, 1900105 (2020).

[68] Y. Kuno, T. Orito, and I. Ichinose, Flat-band many-body localization and ergodicity breaking in the creutz ladder, *New Journal of Physics* **22**, 013032 (2020).

[69] T. Orito, Y. Kuno, and I. Ichinose, Interplay and competition between disorder and flat band in an interacting creutz ladder, *Phys. Rev. B* **104**, 094202 (2021).

[70] J. Janarek, B. Grémaud, J. Zakrzewski, and D. Delande, Quantum boomerang effect in systems without time-reversal symmetry, *Phys. Rev. B* **105**, L180202 (2022).

Supplemental Material:

Ubiquity of the quantum boomerang effect in localized systems

Flavio Noronha¹ and Tommaso Macri^{2,1}

¹Departamento de Física Teórica e Experimental, Universidade Federal do Rio Grande do Norte, Campus Universitário, Lagoa Nova, Natal-RN 59078-970, Brazil

²ITAMP, Harvard-Smithsonian Center for Astrophysics, Cambridge, Massachusetts 02138, USA

I. GENERALIZATION OF THE ANALYTICAL DERIVATION

Some models may fail to meet conditions *(c)* and *(d)* with respect to the operator \mathcal{RT} (see the main text) and still present QBE in real space. One such example is the spin-1/2 interpretation of the Harper-Hofstadter ladder, which was briefly discussed in the main text. Here we further generalize assumptions *(c)* and *(d)* in order to guarantee the QBE in more general models. Conditions *(a)* and *(b)* are kept the same. Though we use the notation of one-dimensional single-particle models, the considerations below are valid in general contexts.

Suppose that in the system under consideration there exists some (anyone) unitary operator \mathcal{U} that commutes with the position operator X and it is such that *(c)* $\mathcal{URT}\{H\}(\mathcal{URT})^{-1} = \{H\}$ and *(d)* the initial state is an eigenstate of \mathcal{URT} , $\mathcal{URT}|\psi_0\rangle = e^{i\theta}|\psi_0\rangle$, $\theta \in \mathbb{R}$. Therefore, using the properties of the operators \mathcal{U} , \mathcal{R} and \mathcal{T} and condition *(d)*,

$$\begin{aligned} \langle x(t) \rangle_H &= \langle \psi_0 | \exp(iH^\dagger t) X \exp(-iHt) | \psi_0 \rangle \\ &= [\langle \psi_0 | (\mathcal{URT})^{-1}] [\mathcal{URT} \exp(iH^\dagger t) (\mathcal{URT})^{-1}] [\mathcal{URT} X (\mathcal{URT})^{-1}] [\mathcal{URT} \exp(-iHt) (\mathcal{URT})^{-1}] [\mathcal{URT} | \psi_0 \rangle] \\ &= e^{-i\theta} \langle \psi_0 | \exp(-i\tilde{H}^\dagger t) (-X) \exp(i\tilde{H}t) | \psi_0 \rangle e^{i\theta} \\ &= -\langle x(-t) \rangle_{\tilde{H}}, \end{aligned} \quad (\text{S1})$$

where we have defined $\tilde{H} = \mathcal{URTH}(\mathcal{URT})^{-1}$. Once $[\mathcal{U}, X] = 0$ we used $\mathcal{U}X\mathcal{U}^{-1} = X$. Using condition *(c)* we can conclude that $\overline{\langle x(t) \rangle} = -\overline{\langle x(-t) \rangle}$ and, in particular,

$$\overline{\langle x(+\infty) \rangle} = -\overline{\langle x(-\infty) \rangle}. \quad (\text{S2})$$

From Eq. (3) in the main text and Eq. (S2) we have

$$\overline{\langle x(+\infty) \rangle} = 0, \quad (\text{S3})$$

which guarantees that the QBE occurs.

The generalization above also applies to the QBE in momentum space. The demonstration is analogous to the ones presented and considers only the operator \mathcal{UT} instead of \mathcal{URT} , where \mathcal{U} commutes with the momentum operator P .

II. QBE IN THE QKR

The proof of the QBE in momentum space is similar to that in real space. Here we use the noninteracting QKR as example for this demonstration and follow some of the steps presented in [46]. In general it is required that *(a)* the Hamiltonian presents dynamical localization, *(b)* all eigenenergies are real, *(c)* $\mathcal{T}\{H\}\mathcal{T}^{-1} = \{H\}$ and *(d)* $\mathcal{T}|\psi_0\rangle = \pm|\psi_0\rangle$. Condition *(c)* is trivially met in the QKR with $\alpha = 1/2$ once the model becomes T symmetric. In this case we can consider that the ensemble $\{H\}$ is composed by only one Hamiltonian H . The QKR does not require disorder to present dynamical localization; instead, the distribution of quasimomenta in $|\psi_0\rangle$ plays the role of pseudo disorder. Therefore there is no need to define the average $\langle \dots \rangle$ in the QKR.

In the case of the QKR, which has a time-dependent Hamiltonian, we can expand $|\psi_0\rangle = \sum_n c_n |\phi_n\rangle$ in terms of the eigenvectors of its Floquet operator, $U|\phi_n\rangle = \exp(-i\epsilon_n t)|\phi_n\rangle$. The eigenstates of U and U^\dagger are identical, and correspond to the eigestates of the same self-adjoint, time-independent Floquet Hamiltonian. At any time $t = l \in \mathbb{N}$, the average momentum is given by

$$\langle p(t = l) \rangle = \sum_{n,m} c_n c_m^* \exp[-i(\epsilon_n - \epsilon_m)l] \langle \phi_m | P | \phi_n \rangle, \quad (\text{S4})$$

where P is the momentum operator. Note that this same expression is expected to hold for other models with a time-independent (Floquet) Hamiltonian that meets condition *(b)*. Condition *(a)* leads to the diagonal ensemble

$$\langle p(t = +\infty) \rangle = \sum_n |c_n|^2 \langle \phi_n | P | \phi_n \rangle. \quad (\text{S5})$$

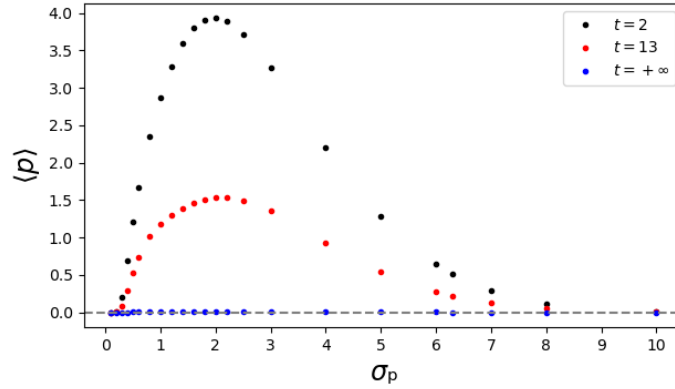


Figure S1. **Dependence of QBE on the initial width of the wave packet.** We propagate the wave function in the non-interacting QKR using Floquet operators as in [43] and used $n = 1000$ values of integer momenta, $n_d = 1000$ values of quasi-momentum β , $x_0 = \pi/2$, $K = 5$ and several values of σ_p .

We stress here that in the QKR the role of disorder realizations is played by the quasimomentum distribution of $|\psi_0\rangle$, which leads to a sufficiently large set of non-zero numbers $\{c_n\}$ that guarantee that the off-diagonal terms cancel out. Other models may require an average $\overline{\dots}$ over a large set $\{H\}$ to ensure the diagonal ensemble. A similar expression holds for $t \rightarrow -\infty$ and then

$$\langle p(+\infty) \rangle = \langle p(-\infty) \rangle. \quad (\text{S6})$$

Following Eq. (4) in the main text, considering \mathcal{T} instead of \mathcal{RT} , the momentum operator P instead of X and defining $\tilde{H} = \mathcal{T}H\mathcal{T}^{-1}$ we find $\langle p(t) \rangle_H = -\langle p(-t) \rangle_{\tilde{H}}$ using condition (d). Therefore, using (c) we find

$$\langle p(+\infty) \rangle = -\langle p(-\infty) \rangle. \quad (\text{S7})$$

From the above relations we have $\langle p(+\infty) \rangle = 0$, which guarantees that the QBE occurs in the QKR.

The above derivation is more general than the one presented in [46] in the sense that here we do not use that the Hamiltonian is parity symmetric; we just use condition (c). We emphasize that the above derivation may remain valid for other models with dynamical localization when considering the average $\overline{\dots}$.

In the QKR the amplitude of the boomerang depends on the width of the initial wave packet. See Fig. S1 for the non-interacting case.

In Fig. S2 we display additional data for the interacting QKR of Eq. (10) in the main text. Using $K = 2$ and $K = 8$ we find evidence for the existence of a critical interaction g_c below which there exists a partial boomerang with a U-turn.

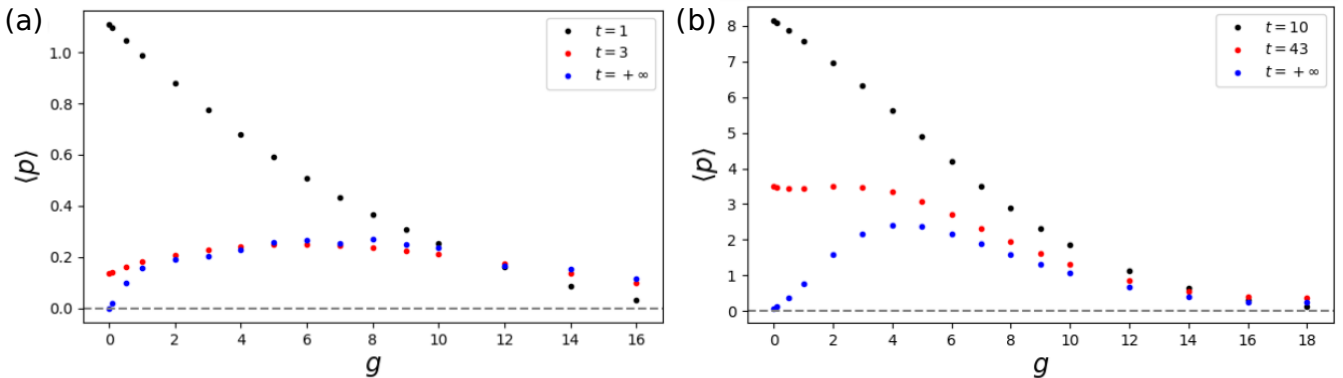


Figure S2. **Partial QBE in the interacting quantum kicked-rotor model.** In (a) we use $K = 2$ and show the average momentum at $t = 1$ (black) and at $t = 3$ (red). In (b) we use $K = 8$ and show the average momentum at $t = 10$ (black) and at $t = 43$ (red). The asymptotic momentum average $\langle p \rangle_{t=\infty}$ is shown in blue and is computed as an average of $\langle p(t) \rangle$ in the interval $t \in [500, 1000]$. For both plots we set $\alpha = 0.5$, $x_0 = \pi/2$, $\sigma_k = 3$, $\bar{k} = 1$, size of the system $L = 2\pi \times 512$, discretization in real space $\Delta x = 2\pi/1024$ and in time $\Delta t = 10^{-2}$.

III. ADDITIONAL DATA FOR THE HARPER-HOFSTADTER LADDER MODEL

If the two chains in the Harper-Hofstadter ladder model are disconnected ($\Omega = 0$), it is possible to use values for the magnetic flux ϕ and momentum k_0 such that the particle propagates in opposite directions in each chain [see Fig. S3(a)]. Using a finite Ω leads to a tendency for the particle to propagate in the same direction in both the chains [see Fig. S3(b)]. When the initial wave packet is nonzero in only one of the chains, a finite inter-lattice hopping Ω allows the particle to partially migrate to the other chain [see Fig. S3(c)]. In all these cases the QBE is present in each chain.

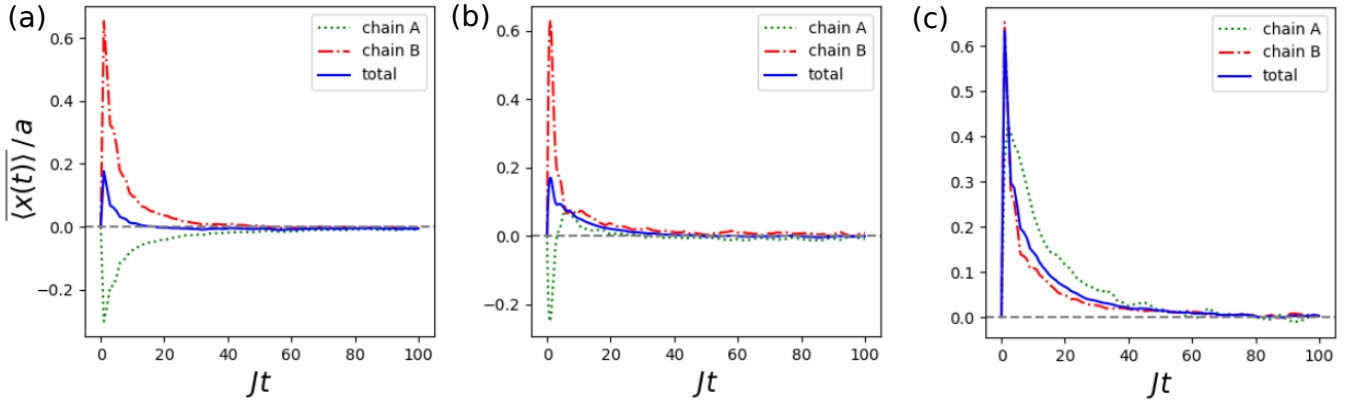


Figure S3. Harper-Hofstadter ladder model. We show the disorder averaged center of mass in chain A (green dotted line), chain B (red dash-dotted line) and averaged in the whole system (blue solid line). We used $W/J = 6$, $N = 2 \times 10^2$, $n_d = 5 \times 10^4$, $\sigma/a = 10$, $k_0a = 0.2$ and $\phi = (\pi/2)(\sqrt{5} - 1)/2$. We show (a) two disconnected chains with $\Omega/J = 0$ and initial state ψ_{0+} , (b) two connected chains with $\Omega/J = 0.3$ and initial state ψ_{0+} , and (c) two connected chains with $\Omega/J = 0.3$ and initial state in chain B only, $(\psi_{0+} - \psi_{0-})/\sqrt{2}$.